CrossMark

ORIGINAL PAPER

Seismically induced slope instability maps validated at an urban scale by site numerical simulations

G. Vessia[1,2] · L. Pisano[1,3] · G. Tromba[4] · M. Parise[1]

Abstract Maps of seismically induced instability at the urban scale can be drawn by means of geographic information system (GIS) tools that integrate different information layers such as (1) a landslide inventory; (2) a digital elevation model (DEM); (3) geo-hydro-mechanical site characterization, and (4) measured peaks or integral parameters at seismic stations. These maps are used to guide planning activities and emergency actions, but their main limitation is typically the lack of reliable analyses or calibrations. In this study, a possible method is proposed to control and increase the overall reliability of an hazard scenario map of earthquake-induced slope instability. The procedure can be summarized in the following steps: (1) GIS tools are used to describe the spatial distribution of the hydro-mechanical properties of the surface lithologies; (2) seismically induced instability maps of permanent displacements are drawn from the preceding information layers combined with seismic parameters spatially propagated by means of spatial interpolation tools; (3) point dynamic and stability numerical analyses are carried out by means of a commercial finite element method (FEM) code (e.g., Geostudio2004) to calculate permanent displacement by the Newmark's method along representative cross-sections. The numerical analyses are used to calculate a "depth factor", which can be considered as the contribution of the seismic local amplification to the surface calculations addressed by GIS tools. The ratio between the results drawn from the two approaches (GIS-based and FEM-based implementing Newmark's method) can be assumed as a scale factor related to the in-depth site-specific geo-lithotechnical characters to be addeded to GIS maps.

Keywords Newmark's method · Seismic permanent displacement · Landslide zonation · Hazard map · Dynamic finite element analysis · 1980 Irpinia earthquake

Introduction

Production of hazard maps by means of geographic information system (GIS) tools is a commonly used approach to address land use planning at large, intermediate and small scales. In particular, at large scale (<1:5000), hazard maps may support emergency and evacuation plans by civil protection service, contributing to address and manage population rescue in the aftermath of natural disasters, e.g., strong earthquakes, floods, and landslides. In this respect, GIS-based maps enable zonation through two-dimensional (2D) spatial interpolating tools by combining several different information layers of spatially distributed data. Further, the use of embedded digital elevation models (DEM) within GIS devices enable calculations concerning shallow landslides, soil erosion, and water infiltration in the first few meters below the ground. Nevertheless, the main limitation of GIS-based hazard studies is they do not account for the influence of variable physical, mechanical

✉ G. Vessia
g.vessia@unich.it

1   Institute of Research for Hydrogeological Protection IRPI, National Research Council CNR, Bari, Italy

2   Department of Engineering and Geology, University "G. d'Annunzio" of Chieti-Pescara, Chieti Scalo, Chieti, Italy

3   Department of Biosciences, University of Molise, Pesche, Isernia, Italy

4   Professional Geotechnical Engineer, Matera, Italy

Springer

and geometrical features of soil and rock in depth. This limitation affects the quality of hazard maps, decreasing as the scale of the study increases. Especially in seismically induced landslide zonations, groundwater and infiltration conditions, soil and rock attitudes and lithotechnical properties in depth heavily affect the quantitative amount of permanent displacements, as calculated by the simplified Newmark's method (Jibson 1993) at urban scales (that is, between 1:5000 and 1:2000). Such limitations have been recognized, discussed and pointed out in the guidelines for landslide susceptibility, hazard and risk zonation for land-use planning edited by Fell et al. (2008a, b). This issue represents the latest milestone in landslide mapping and points out the need for field checks of GIS modeling outputs in order to produce high-quality zonation maps. In this regard, Fell et al. (2008a, b) advise that GIS models must be calibrated in any study, due to the following sources of errors responsible for inaccuracy, among others: (1) spatial variability and uncertainties in subsoil properties (2) poor description of geomorphological evidence of active instability, and (3) geometrical approximations and simplifications in DEMs. They also suggest two possible validation methods: (1) by peer reviewers appointed to provide independent assessment of the susceptibility, hazard and risk zonations (however, this review could be only performed on qualitative bases); (2) for zonation maps based on quantitative parameters or indexes, "through a formal validation by splitting the landslide inventory in two groups: one for analysis and one for validation" (Fell et al. 2008b, p. 95). Moreover, the use of GIS analyst tools cannot substitute, in landslide zonation, the involvement of geotechnical models and parameters to be measured in depth. On the contrary, GIS is an assistant for efficiently accomplishing landslide zoning. According to the advice above, we propose to calibrate quantitative instability maps of seismically induced permanent displacements in urban areas through finite element analyses.

The main focus of this paper is to compare permanent displacements calculated by Newmark's method applied to seismic signals drawn from the 2D dynamic finite element analyses with those from the Newmark's sliding block method formulated for GIS-based spatial analyses. This study is not aimed at dealing with the precision of the two methods, but it highlights whether or not there is a correspondence of results at a site. Differences in the order of magnitude of results could mean that the amplification effects due to the "dynamic soil properties" should be taken into account when GIS-based maps of permanent displacements are drawn. The ratio between the results from the methods is named "depth factor", and can be used as the calibration factor of GIS permanent displacement maps when FEM analyses are applied at the urban scale.

This approach has been implemented hereafter to the case study of the Castelfranci urban area, located in the central sector of the southern Italian Apennine Chain. The village is set in an unstable territory where strong seismic shocks like the 1980 Irpinia earthquake are registered. There, seismically induced permanent displacement maps were drawn by Vessia et al. (2013). Hereafter, two representative cross-sections of the Castelfranci urban area have been modelled by a finite element metode (FEM) commercial code, namely GeoStudio2004 (http://www.geo-slope.com/support/geostudio2004/). Then, permanent displacements along the two numerical models have been calculated and compared with those obtained from the maps.

In the following sections, firstly the main characters of seismically induced landslides on Italian territory are reported. Secondly, both rigorous and simplified formulations of Newmark's sliding rigid block method are summarized. Afterward, the case study of the Castelfranci urban area is introduced and its seismically induced permanent displacement maps calculated by GIS tools are briefly illustrated. Eventually, FEM analyses are proposed to calibrate the GIS-based maps of permanent displacements through a site specific "depth factor".

Main characters of seismically induced landslides in Italy

Seismically induced landslides have been widely described and classified in the last thirty years. Keefer (1984) studied 40 earthquakes with local magnitude M_L ranging from 5.2 to 8.7 that triggered landslides in the USA in the time period 1958–1977. He grouped the observed landslides in three classes: (I) fall and sliding with mass disgregation both in rock and soil; (II) rigid rapid block sliding both in rock and soil and slow earthflows; and (III) lateral spreading, flows and submarine landsliding. Keefer recognized that these categories are commonly initiated by three different minima M_L values that are 4.0, 4.5 and 5, respectively. D'Elia (1992, 1998) investigated the characters of seismically induced landslides having occurred in Italian seismic areas. He found that (1) relevant landsliding phenomena have been triggered by the 1783 Southern Calabria earthquake (7.1 M_W), the 1976 Friuli earthquake (6.4 M_L), the 1980 Irpinia earthquake (6.5 M_L) and the main shock of the long 1997 Umbria-Marche seismic sequence (5.8 M_L) (http://emidius.mi.ingv.it/CPTI15-DBMI15/). (2) Clayey soils and rock masses have only been affected by the aforementioned strong earthquakes. (3) Fall, sliding and earth flows are

the most frequent mass movements displaced on the Italian territory. (4) The 1976 Friuli and the 1980 Irpinia earthquakes reactivated several large dormant landslides, especially planar and rotational slides, mudslides, and earthflows. (5) Distances between the epicenters of the main shocks and the triggered landslides are in accordance with those predicted in wet climates by TC4-ISSMFE 1999, shown in Fig. 1.

Furthermore, D'Elia (1998) studied the mechanical characters of landslides triggered by the 1980 Irpinia earthquake in clayey soil slopes. He pointed out that the landslides showed variable characters in terms of the movement type (slides, flows and complex landslides) and displacement magnitude (from a few centimeters to hundreds of meters). Moreover, the predisposing conditions to movements were the high pore pressures induced by precipitations although the triggering factor was always represented by the inertia forces. Eventually, D'Elia (1998) stated that almost all types of landslides occurred after the soil shear strength was exceeded along distinct weak surfaces.

Landslide phenomena triggered by the 1980 Irpinia earthquake were also studied by several authors through site-specific stability analyses (Dramis et al. 1982; Hutchinson and Del Prete 1985; Cotecchia et al. 1986; D'Elia 1992). Based on these studies, Romeo (2000) recalculated the permanent displacements observed, deriving an attenuation equation that is reported in Fig. 2, where permanent displacements are plotted versus the minimum distance from the ground projection of the fault. It can be pointed out that relevant permanent displacements took place up to 20 km from the surface fault projection.
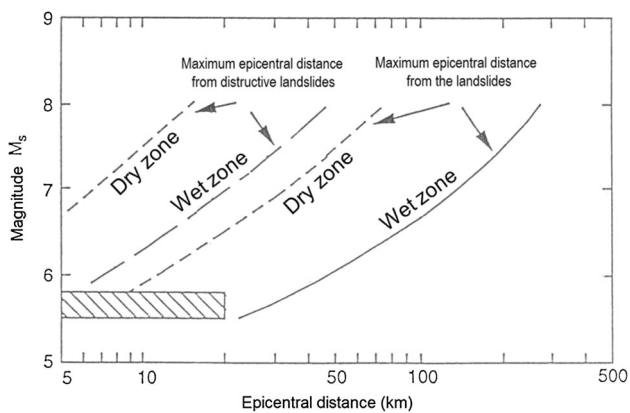

Fig. 2 Relationship between permanent displacements measured at landslide points and the minimum distance to the surficial projection of the fault of the landslide points

Newmark's method to estimate the permanent displacements induced by seismic actions

Newmark's method (1965), known as the "sliding block model", assumes that seismic ground accelerations are transient phenomena generating permanent deformations of the slope, called *permanent displacements*, preceding any significant damage. According to the limit equilibrium slope stability analysis, the landslide mass is assumed as a rigid friction block that is moved downslope by forces exceeding the critical acceleration of the slope. This latter is the value of the ground acceleration at which the slope will get to the ultimate strength, that means the factor of safety FS is equal to one. According to the sketch plotted in Fig. 3, those portions of the accelerogram that exceed the critical acceleration are summed up, and twice integrated to get the total permanent displacements. In doing this, Newmark's method takes into account the strong-motion

Fig. 1 Relationship between magnitude and epicentral distance based on a worldwide database of seismically induced landslides (after TC4-ISSMFE 1999, modified). The dashed rectangle represents the landslides triggered by the main shock of the 1997 Umbria-Marche seismic sequence
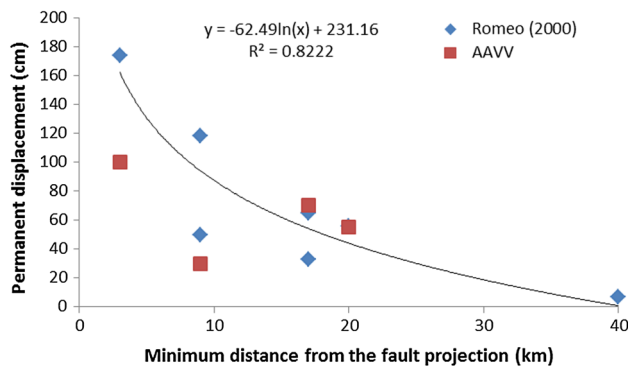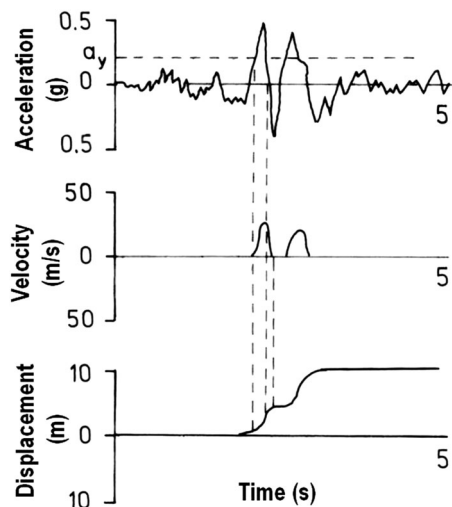

Fig. 3 The three-step Newmark method calculation of permanent displacements

duration and all those acceleration values that are higher than the critical one, even though lower than the peak horizontal acceleration PGA.

Furthermore, the assumption that the sliding mass is a rigid friction block is commonly used not only for translational or rotational slides, but also for earthflow (according to Cruden and Varnes classification 1996). The rigorous Newmark's method has been quantitatively validated by Goodman and Seed (1966) at the laboratory scale, and by Wilson and Keefer (1983) on a natural slope after the Coyote Lake, California, earthquake of 6 August 1979 ($M_L = 5.7$). Concerning this latter experience, the 1979 Coyote Lake earthquake reactivated a slump located on the northeast shore of Lake Anderson and caused a 20-m-long fissure with 27-mm displacement. These displacements were in excellent agreement with those predicted by the Newmark's method.

The validation carried out by Wilson and Keefer (1983) was performed at the landslide scale by a combination of (1) two actual seismic records, (2) field measurements on the slope, (3) estimates of material properties by using laboratory measurements in similar rock types (Wieczorek et al. 1982), and (4) a dynamic numerical model. Anyhow, it is well known that slope deformation models provide only "order of magnitude" predictions or an "index" of the anticipated level of deformation (Strenk and Wartman 2011, and references therein). Thus, the local variations of seismic action (local amplification or deamplification) and soil response must be taken into account in any quantitative estimations of permanent displacement values.

Although the calculation of permanent displacement is commonly assumed as a useful approach to quantify the seismic effect on soil and rock slopes, it is not commonly shared what the critical amplitude of permanent displacements that trigger landslides is. According to Wieczorek et al. (1985), 5 cm can be assumed as the critical displacement value that produces visible cracks into the landslide mass. Keefer and Wilson (1989) assumed 10 cm as the critical displacement for landslides in southern California, whereas Jibson and Keefer (1993) posed critical displacements of 5–10 cm for landslides in Mississippi Valley.

Since Newmark's method introduction, a number of simplified equations to derive permanent displacement from seismic ground motion parameters have been proposed worldwide especially for drawing GIS-based maps (e.g., Franklin and Chang 1977; Sarma 1980; Ambraseys and Menu 1988; Yegian et al. 1991; Jibson 1993, 2007; Ambraseys and Srbulov 1995; Luzi and Pergalani 1996; Jibson et al. 1998; Parise and Jibson 2000; Romeo 2000; Bray and Travasarou 2007; Hsieh and Lee 2011, among others).

The general rule for a simplified assessment of permanent displacements can be written as follows:

$$\log(D) = A \cdot g(s) + B \cdot h(k) + C \pm \sigma, \tag{1}$$

where A, B, C are coefficients of the regression analysis, $g(s)$ is the dynamic action, $h(k)$ is the landslide susceptibility to failure and σ is the standard deviation of the model.

Jibson (2007) addressed a review of previous regression models for calculating the Newmark permanent displacement. According to his study, the formulas take into account four basic factors: PGA or maximum acceleration, Arias intensity I_a, critical acceleration k_c, and earthquake magnitude M. PGA is commonly used to represent the ground-shaking intensity, although it is not distinctive among different acceleration time histories, but it only measures a single acceleration value. The Arias intensity represents the earthquake intensity by the integration of squared accelerations over time. It is strictly related to the energy content of the recorded signal. It has been demonstrated to be an effective predictor of earthquake damage potential relating to the seismic slope stability (Wilson and Keefer 1983; Harp and Wilson 1995). Jibson (1993) suggested to use the Arias intensity, because it measures the total acceleration of the record rather than just the peak value, so providing a more complete characterization of the shaking content of a strong ratio, in good agreement with the Arias intensity. Several other formulas have been derived by researchers, taking into account distinctive parameters of the seismic response at a site, such as Bray and Travasarou 2007. Their seismic displacement model captures the primary influence of the critical acceleration k_c, its initial fundamental period Ts, and the ground motion spectral acceleration at a degraded period equal to 1.5 Ts. This latter period must be estimated case by case and cannot be generalized, even at local scale (e.g., urban or province scale), where different stratigraphic conditions are responsible for the modifications of the "predominant periods" of the input motions. As a matter of fact, local conditions (such as the successions of different soil layers, their variable depth and properties, the variable geometry of boundaries dip between soil layers) play a paramount role in seismic amplification or de-amplification. Thus, Ts is not a piece of information that can be derived from a surficial survey (GIS-based) of hydro-physical–mechanical properties, while it should be related to a number of data that are commonly not available when seismically induced instability maps are drawn for planning activities.

In this study, two different equations will be used to calculate the permanent displacements produced by the 1980 Irpinia earthquake; they are the Ambraseys and Menu (1988) equation, as modified by Jibson (2007):

$$\log D(cm) = -2.710 + \log[(1-k)^{2.335} \cdot K^{-1.478}] + 0.424M \pm 0.454 \tag{2}$$

and the equation proposed by Jibson ([2007](#)):

$$\log D(cm) = 0.561 \log(I_a) - 3.833 \cdot \log(K) \\ - 1.474 \pm 0.616 \quad (3)$$

where K is the ratio of the critical horizontal acceleration normalized to the peak ground acceleration value:

$$K = k_c(g)/PGA(g) \quad (4)$$

Landslide susceptibility to failure is generally expressed by the critical horizontal acceleration k_c, that accounts for slope geometry, geotechnical properties of soils and hydrologic conditions. It is the minimum amount of horizontal acceleration that can bring the slope to the limit equilibrium, that is FS = 1. The empirical relationships conform to the general Eq. ([1](#)):

$$k_c(g) = \frac{(FS - 1) \cdot \tan(\alpha)}{1 + \tan(\alpha) \cdot \tan(\varphi')} g \quad (5)$$

$$FS = \frac{c' + d\left[\gamma_{sat} - m\gamma_w\right]\cos^2(\alpha)\tan(\varphi')}{\gamma_{sat} \cdot d \cdot \sin(\alpha)\cos(\alpha)} \quad (6)$$

where the equation for the safety factor of an infinite slope of soil was formulated by Huang ([1983](#)), where c' and $\varphi'$are, respectively, the effective cohesion and the angle of internal friction of soil according to the Mohr–Coulomb failure criterion, α is the soil slope, d is the failure surface depth and m is the ratio between the water level and the slip surface depth.

The case study of Castelfranci (southern Italy)

Geological and geomorphological features

Castelfranci (Fig. [4](#)) is a village located on the eastern (right) side of the Calore River, flowing in this stretch from south to north. From the geological standpoint, the area shows outcrops belonging to the Miocene Castelvetere Formation, resting unconformably on varicoloured clays, which, in turn, overlie the bedrock, consisting of carbonate platform deposits of the Alburno-Cervati and Maddalena Mts. Unit (Patacca et al. [1990](#); Menardi Noguera and Rea [2000](#); Patacca and Scandone [2007](#)). The Castelvetere Formation consists of turbiditic sandstones, in layers thick from a few centimetres to about 10 m, and chaotic intervals with prevailing clay deposits which include large blocks of variable lithologies (limestones, slates, marls, etc.). The Castelfranci area can be described as characterized by two main lithological complexes (De Vita et al. [2001](#)): the first is prevailingly clay, with presence of calcareous breccias, and inclusions of sandstones and slates; these materials pass laterally to sands and clay silts. On the other hand, the second complex consists of a rhythmic turbidite succession

of bedded sandstones and conglomerates, with a progressive fining-upward sequence leading to massive sandstones. The latter complex crops out along a NW–SE stretch (Fig. [5](#)a), which comprises the upper reaches of the catchments, including the source areas of the main slope movements in the area. The clay complex characterizes the urban area of Castelfranci, and the valley of the Calore River.

As regards geomorphology, the right side of the Calore River is made of low hills, deeply incised by a structurally controlled network of valleys. Relief is on the order of some hundreds of meters, from the highest reaches of the catchments (about 700 m a.s.l.) to the Calore River thalweg (350–400 m a.s.l.). Most of the area is heavily modeled by ancient gravity-related phenomena, whose remnants can be recognized in the upper catchments as old and steep scarps, mainly related to slope movements belonging to the category of rotational slides in their upper reach. Part of these features may re-mobilize, due to several triggering actions, including rainfalls, moderate to strong seismic shocks, and anthropogenic activities (De Vita et al. [2001](#); Vessia et al. [2013](#)). Moreover, the Italian inventory of landslide phenomena produced by the project IFFI (Inventory of Landslide Phenomena in Italy; http://www.pcn.minambiente.it/) (Fig. [5](#)b) highlights the presence of two main landslide bodies named Lago and Chaniello (marked, respectively, with L and C in Fig. [5](#)b). The first has a sliding character within the clayey complex, while the second is classified as mudflow within the sandstone complex of Castelvetere Formation. In addition, within the urban area of Castelfranci, several shallow unstable phenomena take place where the clay complex of the Castelvetere Formation crops out (Fig. [5](#)b). Historical data about landslide movements at Castelfranci are not very abundant. This is quite common in southern Italy, and represents a serious problem when trying to assess the hazard related to slope movements: lack of a sufficient amount of information, and difficulties in ascertaining reliability of the available data (Calcaterra and Parise [2001](#); Glade et al. [2001](#); Gringeri Pantano et al. [2002](#); Calcaterra et al. [2003](#)) typically do not allow to properly define the landslide hazard and risk. At Castelfranci, with the exception of the reactivations related to the 1980 earthquake, all the other dates of landslide activity refer to a rainfall trigger. Notwithstanding the low amount of available data, on the basis of direct testimonies from the inhabitants, it can be stated that the main movements appear to show a quite continuous activity, even though often this does not involve the whole phenomena, but is rather localized in limited sectors of the landslide bodies. A typical example of landslide occurring in prevalent clayey formation at Castelfranci site is the complex slope movement (rotational slide evolving to earthflow) shown in Fig. [6](#). Strictly relating to the urban
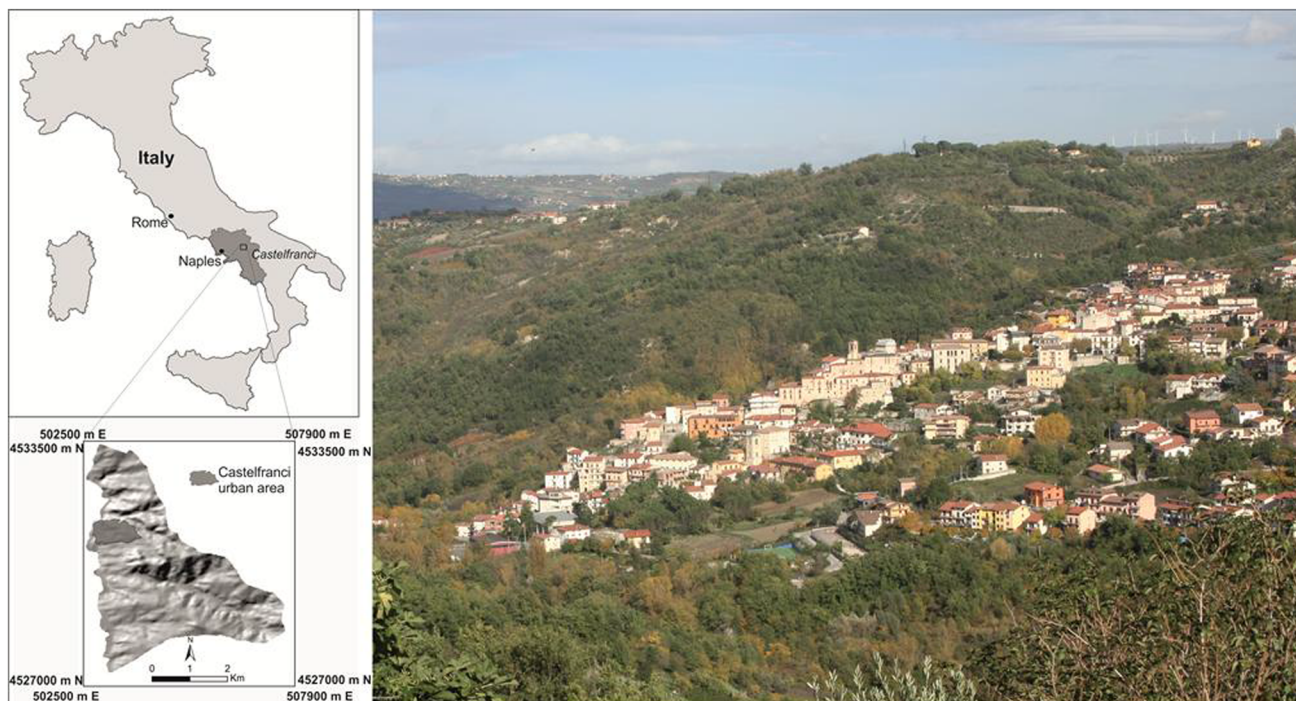
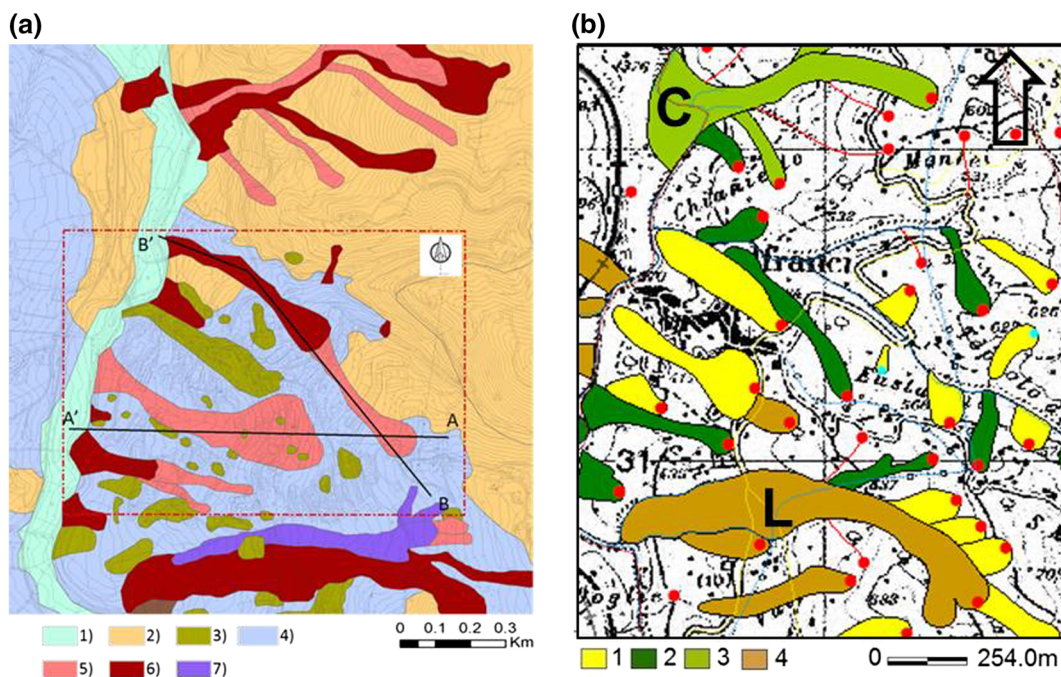**Fig. 4** The Castelfranci village (photo taken from SSW)

Fig. 5 Geological map of the Castelfranci area (modified after Peluso 1998). (*1*) recent alluvial deposits; (*2*) sandstone complex; (*3*) wildflysch olistostromes; (*4*) clay complex; (*5*) dormant landslide; (*6*) active landslide; (*7*) reactivated landslide. The inset in Fig. 5a is the area where we focus in this article (see Fig. 7). *AA′* and *BB′* are the traces of the cross-sections shown in Fig. 8. Figure 5b) IFFI landslide map. Legend: (*1*) translative/rotational; (*2*) earthflow; (*3*) mud flow; (*4*) complex landslide. *L* Lago landslide; *C* Chianiello landslide

area, as shown by Fig. 5b, the slope movements are generally translational slides and earthflows, often originated as a rotational sliding mechanism. Within the built-up area,

due to the presence of urban structures and houses, it is difficult to recognize the single mass movements, which, in any case, produce widespread and almost continuous

Fig. 6 **a** A general view of a typical complex landslide (C in Fig. 5b) at Castelfranci site and **b** a detail of its rotational part, along the left flank

damage. Analysis of the data from field surveys and hydro-geotechnical investigations (discussed in "Geotechnical characterization used in FEM analyses") at Castelfranci indicated that the mass movements are typically shallow, with failure surfaces located at depths greater than 6–8 m.

The area where Castelfranci is located is affected by strong earhquakes generated by the seismogenic zone 927, as defined in the latest Italian Seismogenic zonation ZS9 (MPS Working Group 2004). According to the Italian Macroseismic database DBMI11 (Locati et al. 2011; http://emidius.mi.ingv.it/DBMI11/) the strongest seismic event that struck Castelfranci was the Irpinia earthquake, that occurred on November 23, 1980, at 18:34:53, with a 6.5 M_L (www.itaca.it), at an epicentral distance of about 30 km from the village. This earthquake, besides being among the strongest shocks registered in Italy in recent decades, and with the most severe consequences in terms of casualties and damage, had remarkable effects on the environment, triggering several large landslides (Dramis et al. 1982; Hutchinson and Del Prete 1985; Cotecchia et al. 1986; D'Elia 1992; Parise and Wasowski 1999; Parise 2000).

Multi-temporal analysis

In order to recognise the surface effects produced by the 1980 Irpinia earthquake in the Castelfranci area, and their later evolution, a multi-temporal analysis was carried out by interpreting aerial pictures spanning from 1954 to 1996 (Fig. 7). Landslide activity maps, deriving from the availability and analysis of a multi-year aerial photo coverage, represent a short-cut in the assessment of mass movement hazard, since they focus on the effects of slope instability rather than on the causative conditions and processes (Soeters and van Westen 1996; Parise 2001). Further, when prepared at large scale, they may help the local administrators and land-use planners to reduce the socioeconomic

costs of landslides. Table 1 lists the main features of the aerial photographs used in this study.

In 1954, the landslides in the area appeared very active. This was a quite common situation in large sectors of southern Italy, due to heavy rainstorms in the first years of that decade, which caused a widespread mobilization of landslides. Later on, the state of activity typically slowly decreased, with local activities in a wider scenario of diffuse and old instability (see, in this regard, the outcomes from nearby areas, presented in Parise et al. 2012; Guerriero et al. 2013). Unfortunately, at Castelfranci, no aerial photos before the 1980 earthquake were available to produce a further map, and show such, likely, a decrease. The 1980 earthquake remobilized entirely the main landslide bodies (Chianiello and Lago landslides); in addition, it was able to activate further minor instabilities and landslides, including those that enlarged the main crown area of the Lago landslide (see the 1980 map in Fig. 7). As observed at other landslide sites in the Southern Apennines of Italy (Parise and Wasowski 1999), in the successive years, the activity decreased in some ways, and this can be noted in particular, once again, as concerns the Lago landslide (see the 1990 and 1996 maps in Fig. 7). The Chianiello landslide, on the other hand, remained active, even with some minor source areas feeding the main landslide body from its right flank. Nevertheless, in general, a decreasing trend in the overall landslide activity can be appreciated after the 1980 earthquake. This trend is still occurring nowadays, and involves also the Chianiello landslide, which, at present, shows only local activities, as from the most recent surveys carried out in 2014.

Geotechnical characterization used in FEM analyses

In the Castelfranci urban area, and at its immediate surroundings, several geological surveys and in situ hydrological and geotechnical campaigns have been
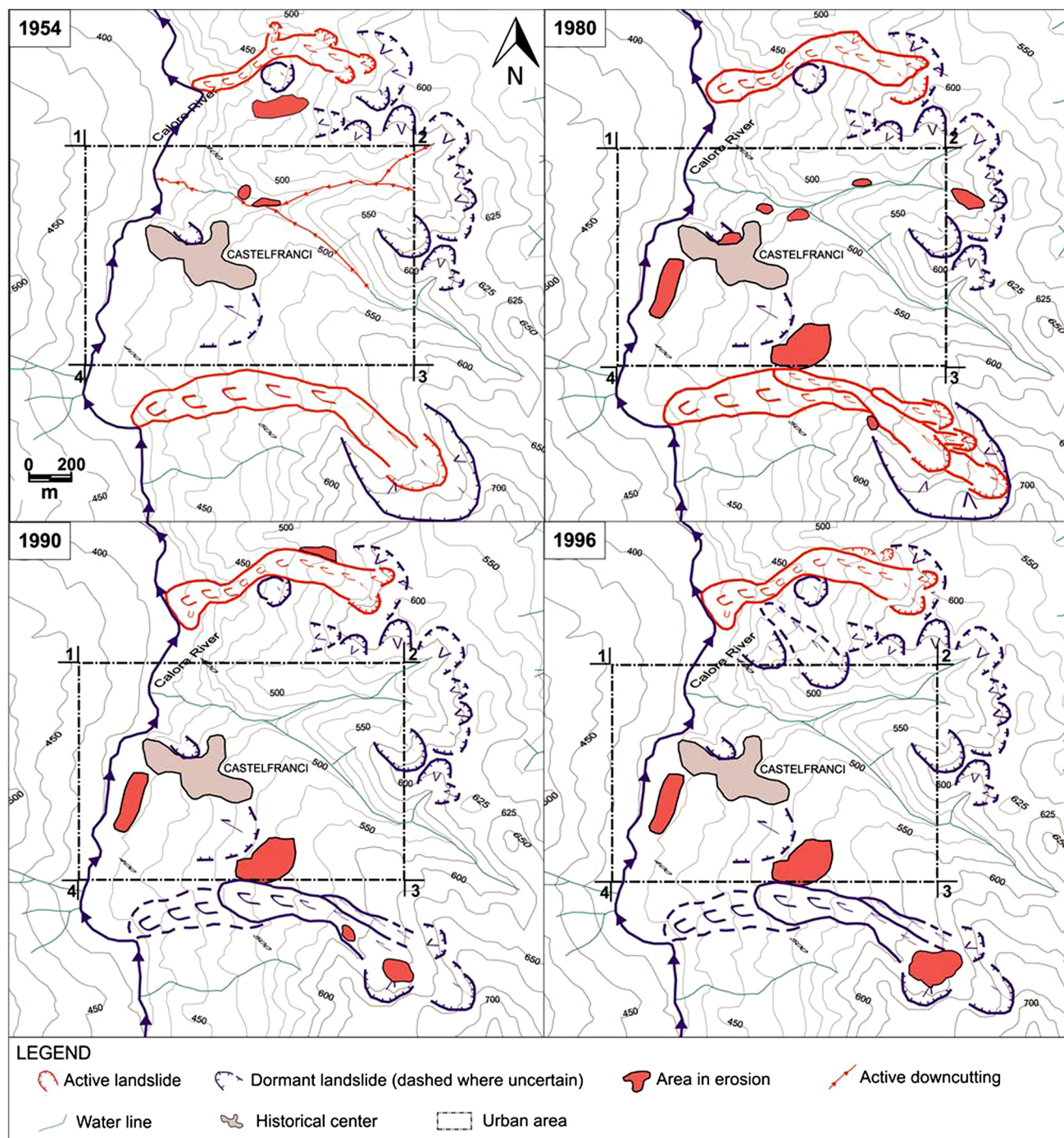
Fig. 7 Temporal analysis of landslide evolution at Castelfranci, performed through analysis of four sets of aerial photographs. UTM coordinates (zone 33T) of the black rectangle edges are: (*1*) 503090 m E, 4531600 m N; (*2*) 504200 m E, 4531600 m N; (*3*) 504200 m E, 4530780 m N; (*4*) 503090 m N, 4530780 m E

performed to derive lithological, hydrogeological, and geotechnical parameter values of local soils and rocks, down to depth of some 30 m. We collected, and critically scrutinized, 40 boreholes where SPT measurements, grain size distributions, down-hole and laboratory shear tests have been executed between 1984 to 2010 by

local professionals (Parise et al. 2014). Commonly, these investigations were undertaken soon after the occurrence (and/or reactivation) of landslide phenomena that threatened buildings and roads. Locations of the collected boreholes is shown in Fig. 8b, where the timing of the surveys is also reported.

**Table 1** Date and average scale of aerial photograph sets used in the study

Date	Scale	Flight height (m)
September 13, 1954	1:33,000	6000
December 05, 1980	1:25,000	2600
June 25, 1990	1:34,000	6000
April 07, 1996	1:40,000	6800

Laboratory shear tests (to measure peak and residual strength parameters) and SPT tests support the identification of a three-layer litho-stratigraphy (entirely belonging to the Castelvetere Fmn.) at Castelfranci, that can be considered as representative for the urban center, as well as for the main landslides, as sketched in Fig. 9 (inset): the first 6 m below the ground level are made up of a weathered clay complex overlying about 10 m of a stiffer sandy-clay complex. The outcropping formation is set on a thick layer of varicoloured clay that locally deepens down to 150 m depth (www.isprambiente.gov.it/Media/carg/450_Santangelodeilombard/fogli.html). Given the depths provided above, the varicoloured clays can be considered as playing the role of a local seismic bedrock for our study area. This latter has been dynamically chracterized by three DHs. P and S wave velocity profiles (respectively, V_P and V_S) have been performed up to 24 and 30 m within the S1, S2 and S4 boreholes (De Stefano 2009; Liotti 2010) (Fig. 8b). Such a depth is not sufficient to characterize the bedrock velocity, although the velocity profiles are able to show that a $V_S \geq 740$ m/s is recorded at depth greater than 10 m. Thus, from the seismic investigations, we drew a conservative seismic stratigraphy consisting of four layers and three lithologies: the shallow weathered clay layer, from the surface to depth of 6 m, shows a mean V_S value of 170 m/s; the second layer of sandy clay, from 7 to 15 m, shows a V_S value of about 500 m/s, while the third layer, the varicoloured clays shows a V_S of 740 m/s at depth from 16 to 30 m, with velocity values reaching at least 860 m/s at greater depths.

In addition, Fig. 7a shows point piezometer measurements within the active portion of the earthflow located near the Calore River, as well as in the vicinity of a dormant translational slide nearby the southern part of Castelfranci. This piezometric campaign has been developed from February 2007 to March 2009 and it shows that the water table level within the weathered clay complex formation has a minimum depth of about 3 m in the fall season, and lowers down to 8 m during the dry period (Liotti 2010). Taking into account that the Irpinia earthquake took place in November, the minimum value of 3 m has been considered for the water table within the FEM dynamic analyses and within the GIS-based maps.

Concerning the simple shear tests performed on 25 samples of the Castelvetere Fmn. drilled to depth of 15 m, a throughout discussion of the variability of cohesion and friction angle values is accomplished in Vessia et al. (2013); here, a brief summary of the lithotechnical parameter values considered in the study is listed in Table 2. This table shows different strength values that have been considered for the intact clay and sandy-clay complexes, compared to the clays involved in the landslide masses. These values are derived by selecting the measured properties according to their depth and the location of the boreholes.
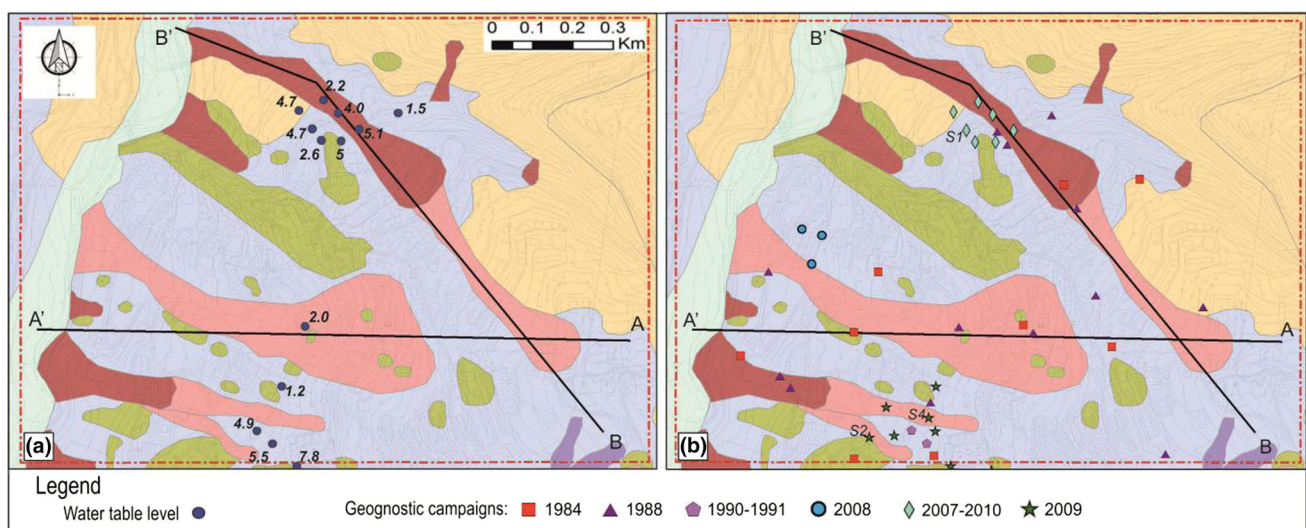
Fig. 8 Water table depth (**a**) measured at Castelfranci in the time span 2006–2010, and boreholes drilled in the time span 1988–2010 (**b**). The *red dashed* line corresponds to the *black rectangle* in Fig. 7
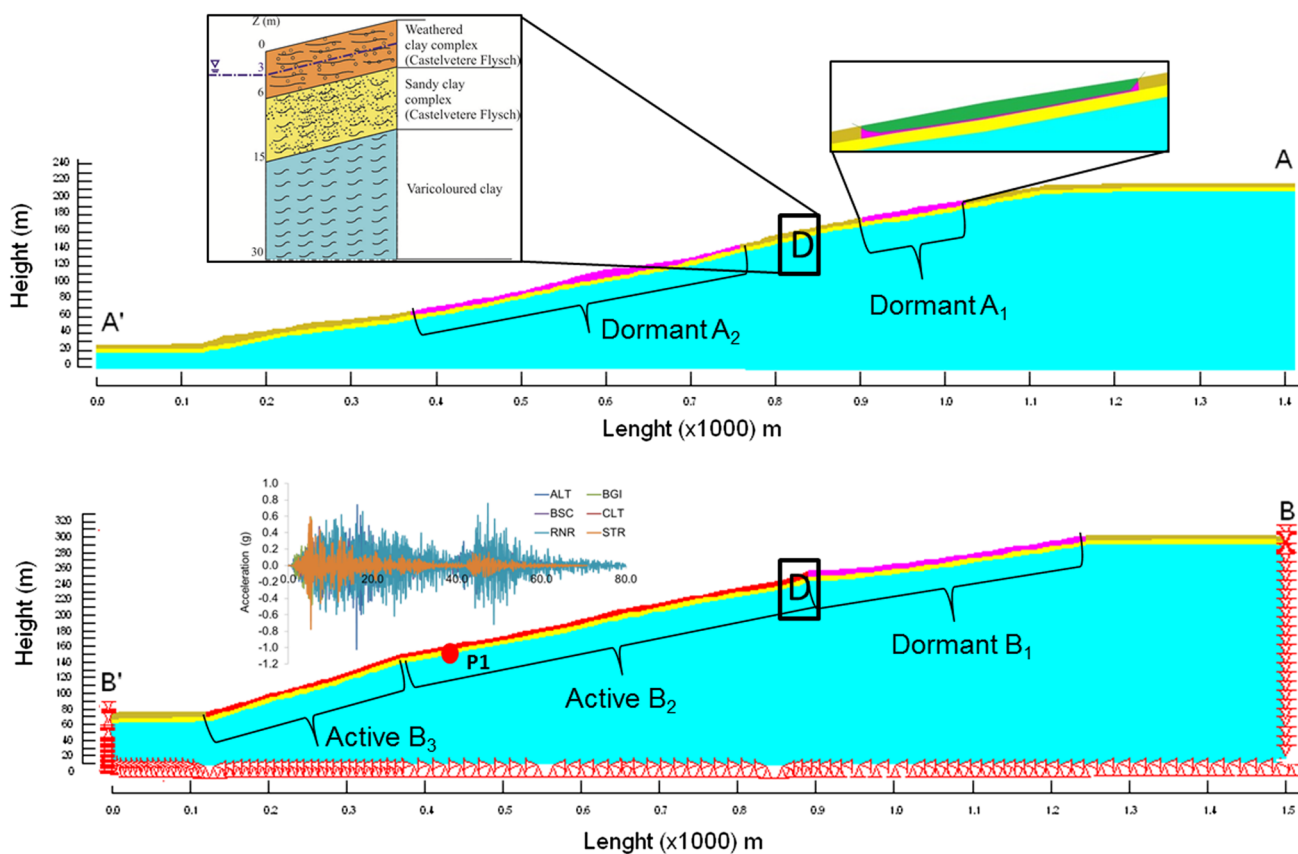
Fig. 9 Cross-sections AA' and BB' used in FE models and stratigraphic details of the first 30 m along the two representative slopes

Table 2 Geotechnical properties of lithotypes at Castelfranci urban center

Lithology	c' (kPa)	ϕ' (°)	γ (kN/m³)	Depth (m)
Sandstone complex (Castelvetere Fm.)	20	28	21	0–6
Weathered clay complex (Castelvetere Fm.)	15	18	17	0–6
Sandy clay complex (Castelvetere Fm.)	20	19	19	6–15
Varicoloured clay	63	23	21	>15
Olistostromes	100	40	26	–
Landslide				
Active landslide in clay	0	14	17	6
Dormant landslide in clay	5	14	17	6
Dormant landslide in sandstone	15	25	18	7

As regards the varicoloured clays, the investigation campaigns at Castelfranci present very few data deeper than 15–20 m. Monaco and Capobianco (2007) carried out some stability analyses under static force conditions, outside the Castelfranci urban area, and used the values listed in Table 2 for the varicoloured clays, on the basis of heuristic knowledge. These values were also later confirmed by Liotti (2010), who performed stability analysis on translational slides located in the Castelfranci village.

In this work, the varicoloured clays were not considered in the stability analyses, because the studied landslides present their sliding surfaces at about 6 m depth (Peluso

1998; De Stefano 2009; Liotti 2010). Nonetheless, the varicoloured clays are considered as the seismic bedrock in the dynamic FEM analyses. Thus, their static mechanical behaviour according to Mohr–Coulomb failure criterion is characterized by the values listed in Table 2, whereas their dynamic parameters are derived by V_p and V_s measurements (Table 3). It is worth noting that beyond a 30-m depth, no dynamic values were available from past investigations. The two sections, AA' and BB', modelling the two slopes and their mass movements were deepened to the geological bedrock. We assumed varying velocity values for V_s: 740 m/s up to 30 m and 860 m/s from 30 m up to

Table 3 P and S wave velocities measured along three drillings within the clay complex of Castelvetere Fmn

Down hole (DH)	Depth (m)	P wave velocity (m/s)	S wave velocity (m/s)
DH1-2010 (S1)*	0–6	328	170
	6–15	863	498
	15–30	1216	860
DH2-2009 (S2)*	0–9	340	217
	9–24	1020	740
DH3-2009 (S4)*	0–9	423	228
	9–24	1086	806

* As reported in Fig. 5

Table 4 Dynamic parameter values used within the time domain FE analyses on the two cross sections AA′ and BB′

Lithology	Depth (m)	Vs Wave velocity (m/s)	Dynamic shear modulus G_0 (MPa)	Dynamic Young's modulus E (MPa)	Unit weight (kN/m³)	Dynamic Poisson coefficient
Weathered clay complex	0–6	170	49.13	184	17	0.35
Sandy clay complex	7–15	500	475	1250	19	0.32
Varicoloured clay	15–30	740	1150	2738	21	0.25
Varicoloured clays	31–bottom	860	1480	3700	21	0.25

the bottom of the two sections. Such an assumption, even though highly conservative at a first glance, does not introduce any ficticious impedance contrast that can generate amplification effects within the seismic bedrock. Finally, all the dynamic parameter values used within the FEM analyses are listed in Table 4.

Permanent displacement maps

The 1980 Irpinia earthquake ($M_L = 6.5$; $Mw = 6.9$) is used as scenario earthquake at Castelfranci to draw GIS-based maps of permanent displacements (Vessia et al. 2013). Castelfranci is located about 30 km from Laviano, which is the epicenter of the main shock (Fig. 10). The peak ground acceleration (PGA) used for drawing the permanent displacement maps was calculated through the ArcGIS10 spatial interpolation tool (Esri Italia 2010). Twenty seismic stations recorded three component signals of the main shock on November 23, 1980 (Fig. 10). Starting from the PGAs and Arias intensity I_A recorded at those stations, by applying the natural neighbouring interpolation method (Sibson 1981), almost constant values of PGA of 0.2 g and I_A of 78 cm/s are assumed at Castelfranci. Moreover, a 10 m-cell size grid DEM from Tinitaly project (Tarquini et al. 2007) was used to calculate the permanent displacement maps. Figure 11 shows the safety factor map FS calculated by Eq. (6). It can be noted that the FS values are almost higher than one, which means that Newmark's method can be applied to the Castelfranci

urban area. A few small areas are characterized by FS ≤ 1, but their limited areal extention does not affect the permanent displacement calculations. The permanent displacement maps are shown in Fig. 12: in detail, Fig. 12a is drawn based on Eq. (2), while Fig. 12b on Eq. (3). The plotted permanent displacement values point out that:

(a) Seismically induced instability can be detected within active landslides both in the clay and the sandstone complexes, as well as in stable areas characterized by steep slopes.

(b) The expected unstable areas, from both the used equations, show the highest displacements (in the range 50–70 cm), whereas the stable areas and the dormant landslides show limited sectors with about 5-cm displacements.

(c) Permanent displacements have been calculated by means of two empirical relationships suggested by Jibson (2007), that use different variables: respectively, I_A and PGA. Within the urban area, slight differences can be appreciated on the predicted permanent displacements.

These results must be interpreted through past seismic experiences in order to associate the calculated values to the actual damages suffered by different types of structures. According to Crespellani et al. (1990), strong damage in urban structures and infrastructures can be generated when displacements are greater than 5 cm; conversely, Bray and Travasarou (2007) suggest considering moderate damage
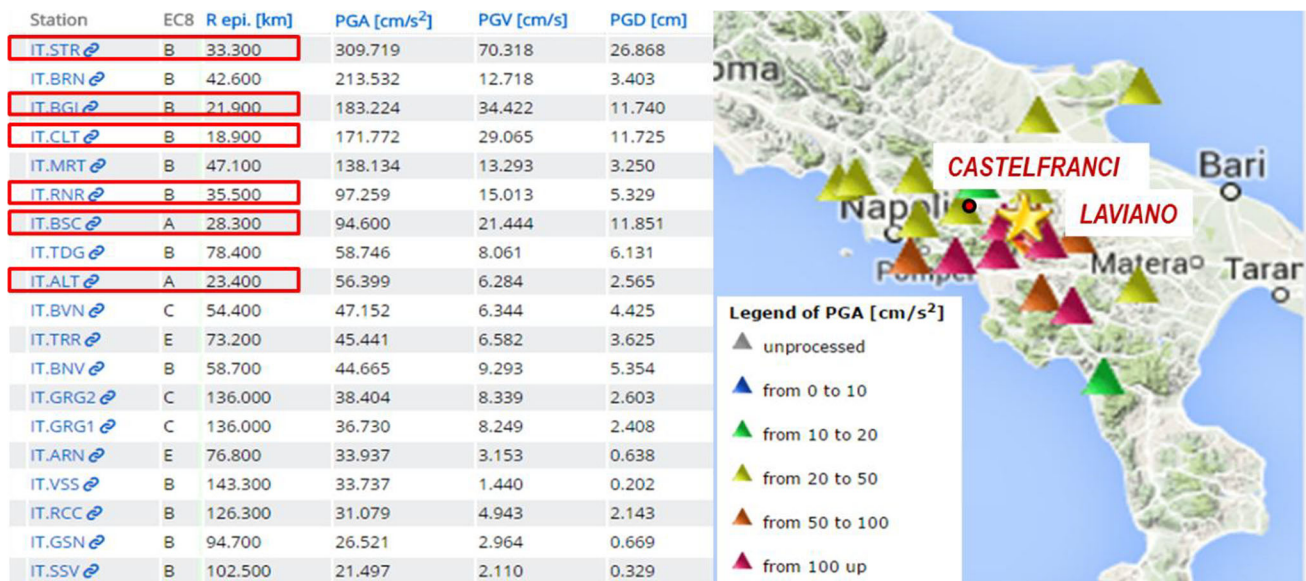
Station	EC8	R epi. [km]	PGA [cm/s²]	PGV [cm/s]	PGD [cm]
IT.STR	B	33.300	309.719	70.318	26.868
IT.BRN	B	42.600	213.532	12.718	3.403
IT.BGI	B	21.900	183.224	34.422	11.740
IT.CLT	B	18.900	171.772	29.065	11.725
IT.MRT	B	47.100	138.134	13.293	3.250
IT.RNR	B	35.500	97.259	15.013	5.329
IT.BSC	A	28.300	94.600	21.444	11.851
IT.TDG	B	78.400	58.746	8.061	6.131
IT.ALT	A	23.400	56.399	6.284	2.565
IT.BVN	C	54.400	47.152	6.344	4.425
IT.TRR	E	73.200	45.441	6.582	3.625
IT.BNV	B	58.700	44.665	9.293	5.354
IT.GRG2	C	136.000	38.404	8.339	2.603
IT.GRG1	C	136.000	36.730	8.249	2.408
IT.ARN	E	76.800	33.937	3.153	0.638
IT.VSS	B	143.300	33.737	1.440	0.202
IT.RCC	B	126.300	31.079	4.943	2.143
IT.GSN	B	94.700	26.521	2.964	0.669
IT.SSV	B	102.500	21.497	2.110	0.329

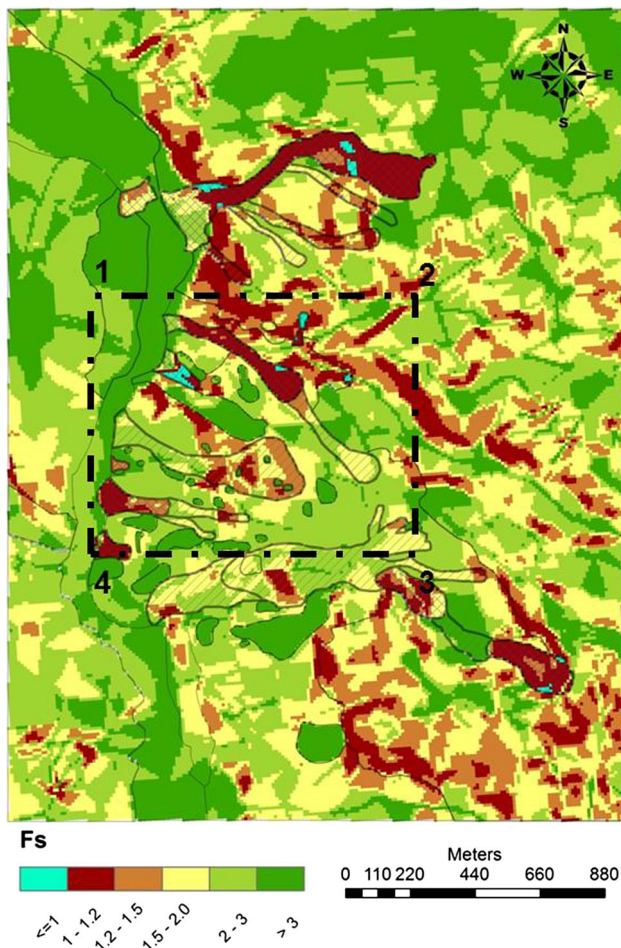**Fig. 10** Seismic stations considered for the input records in the FEM analyses

Fig. 11 Safety factor map calculated by Eq. (6) used within critical acceleration formula k_c, namely Eq. (5). Coordinates of the inset are the same as in Fig. 7 (see corresponding caption)

generated by displacements ranging between 15 and 100 cm. Details on these classifications are provided in Vessia et al. (2013). As cited in "Newmark's method to estimate the permanent displacements induced by seismic actions", Wieczorek et al. (1985) and Keefer and Wilson (1989) suggest 5–10 cm to be the critical displacement values producing visible cracks into the landslide mass. Such values were experienced by the cited authors on the ground; on the contrary, GIS maps drawn from our study are delivered through a simplified model of the territory that did not take into account the amplification effects on seismic shaking of the surficial soil deposits. To this end, local seismic response analyses have been carried out by means of the finite element method. Results in terms of permanent displacements calculated by the following analyses alongside two representative cross-sections of the Castelfranci urban area will be compared with those from the GIS-based maps calculated by Eq. (2) and (3).

FEM local seismic response combined with Newmark's method for permanent displacement calculation

Two representative cross sections (shown in Fig. 8a) have been traced for this analysis along landslides in the Castelfranci area: section AA′ is traced along a dormant translational slide, whereas section BB′ deals with a complex mechanism made up of an active earthflow, superimposed over a translational dormant slide body (Fig. 9). While the first section includes dormant landsliding areas, and a small portion of stable land as well, BB′ covers both the active and dormant portions of the landslides. These two sections are
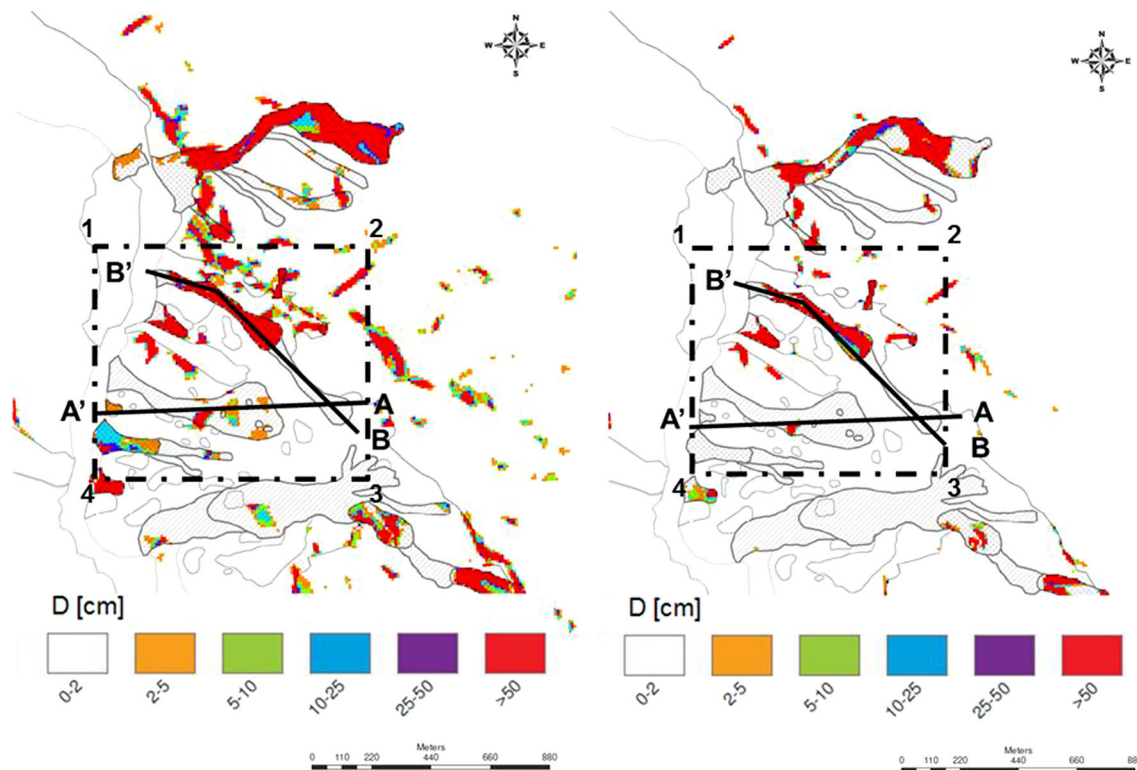
Fig. 12 Permanent displacements calculated by means of simplified formulation of Newmark's method (modified after Vessia et al. 2013): on the left, the Ambraseys and Menu equation, modified by Jibson (2007) was used; on the right, the Jibson formulation (2007) was applied. Coordinates of the inset are the same as in Fig. 7 (see corresponding caption)

mechanically characterized by geotechnical laboratory and in-field tests that were performed by local professionals in their vicinity for monitoring the stability of roads and other human infrastructures. According to the geotechnical and seismic characterization ("Geotechnical characterization used in FEM analyses"), two FEM numerical models have been analysed by GeoStudio2004 suite (GEO-SLOPE international 2004): The dynamic module, namely QUAKE/W, has been used to perform the local seismic response (RSL), and the stability module SLOPE/W has subsequently been implemented on the RSL results to calculate the permanent displacements along shallow sliding surfaces at a 6-m depth.

To compute the permanent displacements, the Newmark's method has been used and applied along the five sliding surfaces shown in Fig. 9 (section AA′). These surfaces have been fully assigned by the operator based on inclinometer measurements and geological surveys developed in the study area ("Geotechnical characterization used in FEM analyses"). For the dynamic analyses, the horizontal signals recorded at the 6 seismic stations indicated in Fig. 10, and characterized by epicenter distance of about 30 km, have been considered. This approach is aimed at considering wave shapes similar to those that reached the site of Castelfranci during the 1980 earthquake. The six

input horizontal accelerograms were scaled to 0.2 g, that is the PGA calculated by the natural neighbor spatial interpolation method implemented within the ArcGis10 code and performed by Vessia et al. (2013). This value has been used in the FEM analyses as the reference PGA (the peak value used for scaling the six accelerograms) on the seismic bedrock, at the bottom of the two cross sections in Fig. 9. This PGA value was actually recorded at 6 seismic stations where the first 30 m of soil deposits are classified as A and B soils (see Fig. 10) according to Eurocode 8 and Italian building code (DM 2008). Nonetheless, the Castelfanci urban area shows a soil type E that is able to amplify the seismic waves through a stratigraphic coefficient S_S equal to 1.528 (DM 2008). The present FEM dynamic analyses is accomplished instead of using the S_S value. Rectangular finite element meshes have been used for the two sections. The boundary conditions applied on the three boundaries of the two FEM models for the dynamic analyses are as follows (Fig. 9b): (1) horizontal x and vertical y null displacements at the bottom of the section, and (2) null y displacement on the vertical cut-off sections. Dynamic analyses have been performed in time domain; thus, accelerograms have been assigned to the bottom of the cross models and relative stress–strain conditions induced by the seismic action have been calculated.

Commonly, the cut-off boundaries are moved away from the portion of the section where numerical results are looked for. To address this task, some trials have been done to verify the horizontal extention of the model influenced by the vertical boundary conditions. After the model calibration, the vertical cut-off boundaries have been moved 120 m from the left side and 300 m from the right side.

The rectangular finite element mesh has a maximum size of both base and height L that fulfills the numerical requirement below:

$$L \leq \frac{V_S}{8 \cdot f_{max}} \qquad (7)$$

where f_{max} is the cut-off frequency (assumed 15 Hz), that is the highest frequency value to be filtered by the physical domain, and V_S is the shear wave velocity of the soil layer (or the region) to be meshed. Parameter values used in the two sections assumed for the three layers are summarized in Table 3. The dynamic time-domain FEM analyses have been performed by means of the QUAKE/W module, assuming an equivalent linear dynamic behavior for the three soil types. Neither degradation curves of the shear modulus $G(\gamma)/G_0$, or the damping ratio curves $D(\gamma)$ are available at the Castelfranci site for either the Castelvetere Formation or varicoloured clays. Nonetheless, we used the laboratory determination of the Atterberg limits (De Stefano 2009) to select the needed curves from literature. The upper weathered clay complex shows a mean plasticity index IP equal to 15, whereas the sandy clay below shows IP about 10. The varicoloured clays have IP < 10. Thus, according to the plasticity index values, G/G_0 and $D(\gamma)$ curves suggested by EPRI (93) for PI = 10 are used for the first two layers of Castelvetere Formation. For varicoloured clays, down to depth of 80 m, the curves EPRI (93) for PI = 10 are used, whereas EPRI (93) ranges between 80 and 150 m are used at depths deeper than 80 m (Fig. 13). The use of the shear modulus degradation curves at depths greater than 80 m is needed in order to not consider a linear constitutive law for the dynamic behavior of the varicoloured clays (actually, no experimental data are available for these stiff soils to provide clues of a linear behavior). This assumption is necessary to propagate the input motion from the bottom of the numerical model to the surface.

Results from FEM dynamic analyses are provided with the accelerograms on the sliding surfaces of the five landslide bodies identified along the two sections AA′ and BB′ (Tables 6, 7). These sliding surfaces are planar and fully defined at a 6-m depth, according to the in-field measurements ("Geotechnical characterization used in FEM analyses").

Considering the point belonging to the sliding surface B2 (Fig. 9), it is worth noticing that the PGA is much
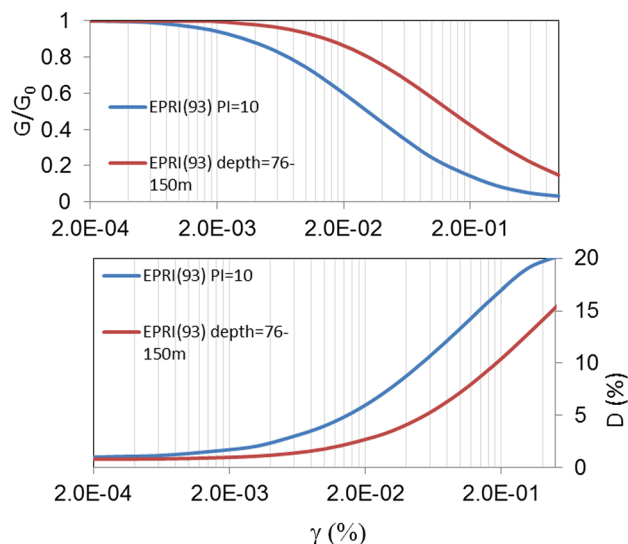

Fig. 13 Shear modulus degradation curves and damping curves for low plastic clay soil (IP = 10) and deep clay soil ranging between 76 and 150 m (after EPRI 93)

Table 5 Critical accelerations k_c calculated along the planar sliding surfaces belonging to section AA′ and BB′

Parameter	A1	A2	B1	B2	B3
k_c	0.18	0.08	0.33	0.13	0.05
DF	25	10	2	2–3	3–5

higher than 0.2 g, thus the amplification effects exherted by the varicoloured clays and the lower sandy complex of the Castelvetere Formation will be taken into account in Newmark's method calculation. As illustrated in Fig. 3, Newmark's method compares the accelerograms to the critical acceleration k_c (calculated by Eq. 5 and listed in Table 5). For the point considered along the sliding surfaces, at first, an average acceleration time-history is computed then the factor of safety (FS) is calculated. After that, five k_c values for all the sliding surfaces are determined through Eq. (5). Hence, those portions of the accelerogram overcoming the k_c value are integrated twice over the corresponding time span. Results from these calculations are reported in Tables 6 and 7.

Discussion of results

Along section AA′, where dormant sliding bodies are present, permanent displacements equal to, respectively, 57 and 71 cm are calculated. Comparing these values to those in Fig. 12, it is evident that an order of magnitude can be assumed as the ratio between the results of the FEM

Table 6 Permanent displacements (cm) alongside the cross section AA′ at Castelfranci calculated by combining the dynamic GeoStudio2004 FEM analyses and Newmark's rigid sliding block approach

| Seismic station	Sliding surface A1	Sliding surface A2
ALT	16	59
BGI	85	58
BSC	93	40
CLT	76	112
RNR	59	120
STR	13	38
Mean permanent displacements	57	71

Table 7 Permanent displacements (cm) alongside the cross section BB′ at Castelfranci calculated by combining the dynamic GeoStudio2004 FEM analyses and Newmark's rigid sliding block approach

Seismic station	Sliding surface B1	Sliding surface B2	Sliding surface B3
ALT	0.7	56	146
BGI	7	52	88
BSC	0.3	285	354
CLT	17	320	375
RNR	0.14	128	335
STR	0	38	115
Mean permanent displacements	4	147	236

analysis along section AA′ and the maps calculated through Eqs. (2) and (3). These differences are strictly related to the local amplification effects shown by the accelerograms in Figs. 14 and 15 that are recorded along the sliding surfaces. The accelerograms show PGAs that are from two to four times the reference PGA (0.2 g) used for GIS-based calculations of permanent displacements. The peaks are higher along section AA' than along BB'. This evidence is reflected in calculated permanent displacements: along the sliding surface B1 they are twice those calculated in Fig. 12 (on the left). Accordingly, permanent displacements along B2 and B3 sliding surfaces show a ratio ranging from twice to five times the GIS-based calculations. These differences can be attributed to the local amplification of the seismic waves and to the critical acceleration values. Looking back to Table 5, where k_c values are shown for each sliding surface, it can be noted that lower permanent displacements are recorded where higher k_c values are calculated. Nevertheless, the number of acceleration ordinates higher than k_c has a paramount role on the total amount of final permanent displacements. It is evident that on k_c values the local variations of the slope angles has a relevant role. In GIS calculations carried out by Vessia et al. (2013), the slope angles were smoothed by the 10-m cell grid DEM used although the present FEM analyses show that this approximation is heavily worsened by neglecting the local seismic amplification along the slopes that can be calculated only through 2D numerical

analyses. Comparing the spatial distribution of the two sets of permanent displacements, it can be stated that GIS calculations are in very good agreement with the FEM results combined with Newmark's method analyses, especially in the case of the Ambraseys and Menu equation (Fig. 12, on the left; Tables 6, 7). In particular, differences between permanent displacements calculated along the A1 and A2 surfaces can be appreciated in Fig. 12 on the left. A full agreement, instead, is observed along the three surfaces of the BB' cross section: B1 suffers very small displacements and it is stable as in Fig. 12, while B2 and B3 suffer very large movements according to the GIS calculations along the active portion of the earthflow in Fig. 12. Thus, the discussed results of the present study enable us to state that FEM analyses confirm the reliability of the spatial distribution of permanent displacements calculated by a simplified equation derived by the Newmark's method. These numerical analyses are needed indeed to calibrate the GIS-based maps in terms of quantitative predictions. To this end, for each sliding surface a "depth factor" (DF) has been calculated and listed in Table 5. It is worth noting that where dormant landslide bodies are located, as in the case of section AA', DF shows higher values than in the BB' section where the major portion of sliding surfaces are related to active landslide movements. Thus, the higher the contribution of soil strength to the slope stability, the higher DF, which stresses the need to use the proposed calibration procedure by FEM analyses.

Fig. 14 Average acceleration (g) vs. time (s) calculated at the sliding surfaces of cross section AA'
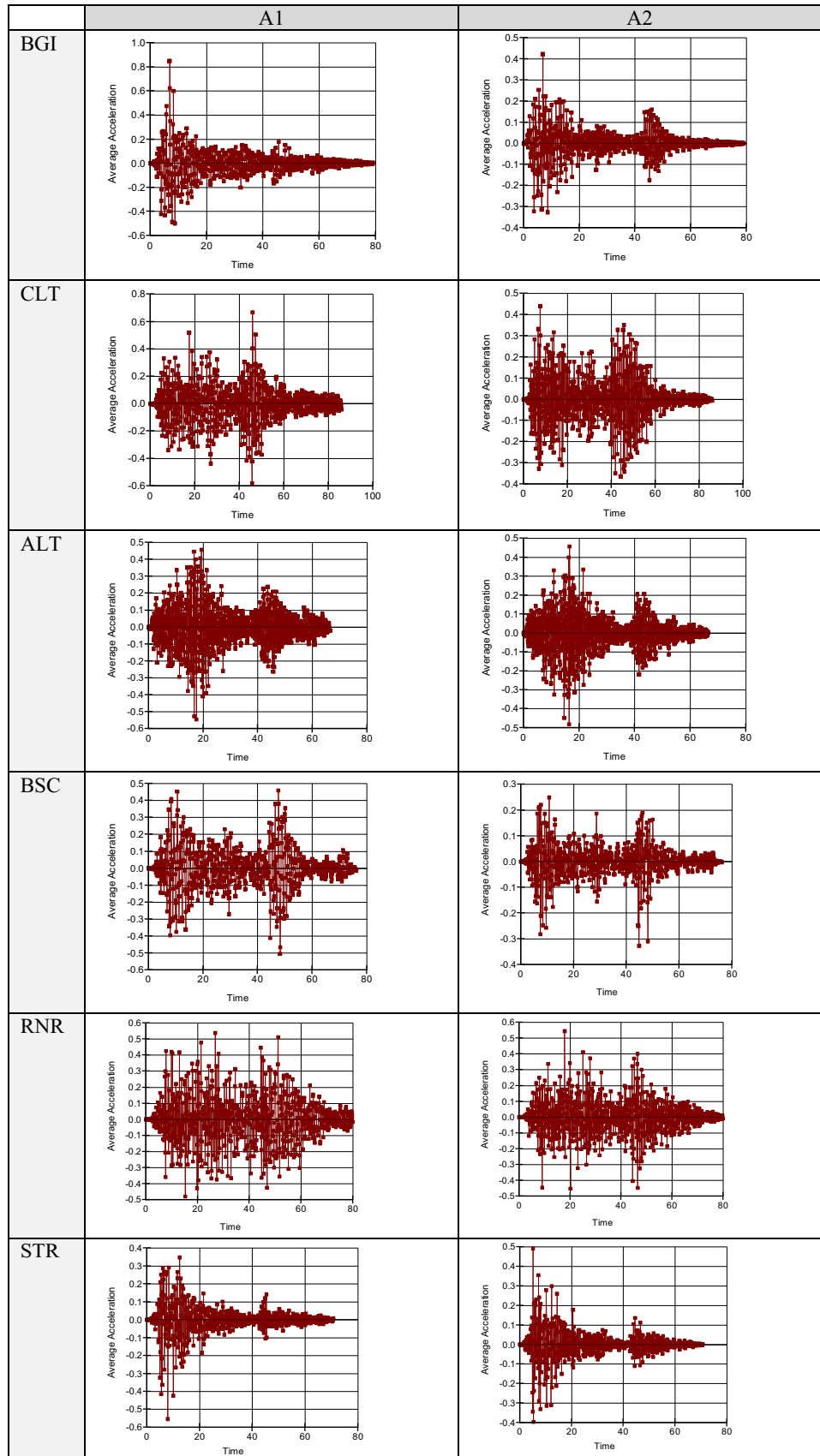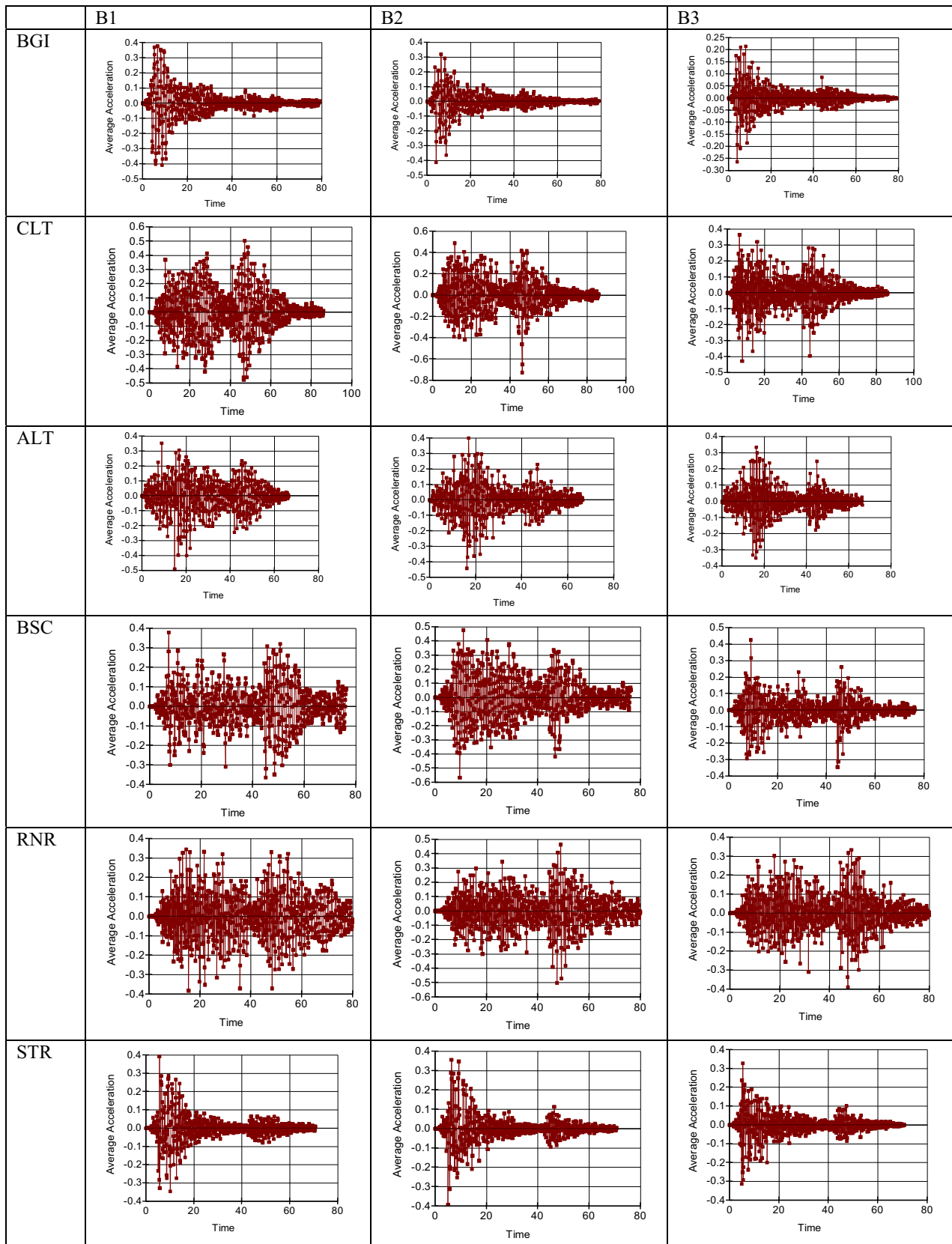
Fig. 15 Average acceleration (g) vs. time (s) calculated at the sliding surfaces of cross section *BB'*

Concluding remarks

In the present paper, the combined calculation of RSL by FEM analyses and the permanent displacements carried out through the Newmark's method is proposed to check the reliability of GIS-based maps of seismic slope instability. Permanent displacement calculations carried out through spatial interpolation tools and simplified equations derived by Newmark's sliding block method have been also calibrated thorugh the proposed DF. The proposed procedure enables checking of the capacity of GIS-based calculations to reliably show the most dangerous areas in terms of seismically induced permanent displacements on slopes, at the urban scale. In addition, at all the sites where soil mechanical characterization is available, the proposed procedure enables calculation of a calibration factor, named depth factor (DF), which takes into account the local contribution of seismic amplification of soil deposits along depth and their resistance to seismic actions depending on the slope angle and their frictional and cohesive strength. From the case study of Castelfranci, two different representative sections have been studied. It was clearly drawn that GIS maps are quantitatively more accurate when applied to soil deposits showing residual strengths. Conversely, these maps must be calibrated by site-specific numerical analyses whenever higher strength values are measured by geotechnical investigation campaigns. Further case studies characterized by different soil and rock types, layer dippings, mechanical shear strenghts and sliding mechanisms must be investigated. As a matter of fact, the resulting effects of the combination of the preceding factors on the seismically induced slope instability cannot be predicted in advance without considering both FEM and GIS-based calculations. In this respect, the two methods can be considered complementary: the FEM results provide a local calibration of GIS-based analyses that, on the other hand, only take into account the surficial "site" conditions. Further studies are needed to check whether generalizations on the "depth factor" could be accomplished and used in typical geo-lithological settings of the Italian national territory and worldwide.

References

Ambraseys NN, Menu JM (1988) Earthquake-induced ground displacements. J Earthq Eng Struct Dyn 16:985–1006

Ambraseys NN, Srbulov M (1995) Attenuation of earthquake-induced displacements. J Earthq Eng Struct Dyn 23:467–487

Bray JD, Travasarou T (2007) Simplified procedure for estimating earthquake-induced deviatoric slope displacements. J Geotech Geoenvir Engrg 133(4):381–392

Calcaterra D, Parise M (2001) The contribution of historical information in the assessment of landslide hazard. In: Glade T, Albini P, Frances F (eds) The use of historical data in natural hazard assessments, advances in natural and Technological hazards research, 17, Kluwer Academic Publishers, p 201–217

Calcaterra D, Parise M, Palma B (2003) Combining historical and geological data for the assessment of the landslide hazard: a case study from Campania, Italy. Nat Hazards Earth Syst Sci 3(1/2):3–16

Cotecchia V, Del Prete M, Tafuni N (1986) Effects of earthquake of 23rd November 1980 on pre-existing landslides in the Senerchia area (southern Italy). Proc Int Symp on Eng Geol Probl Seismic Areas IAEG April 13–19, Bari Italy 4: 4:177–198

Crespellani T, Ghinelli A, Madiai C, Vannucchi G (1990) Analisi di stabilità dei pendii naturali in condizioni sismiche. Riv Ital Geotec 24(2):49–74

Cruden DM, Varnes DJ (1996) Landslide Types and Processes, Special Report. Transp Res Board Nat Acad Sci 247:36–75

D'Elia B (1992) Dynamic aspects of a landslide reactivated by the November 23, 1980 Irpinia earthquake (Southern Italy). Proc. of the French-Italian Conference on slope stability in seismic Areas, Bordighera, p 25–32

D'Elia B (1998) Stabilità dei pendii in zona sismica. Atti del corso di Ingegneria geotecnica sismica, Pesaro. (**in italian, hard copy only**)

De Stefano A (2009) Studio geologico-tecnico finalizzato all'accertamento delle condizioni generali di stabilità in funzione del rischio frane, sismico e delle caratteristiche geomeccaniche dei litotipi fondali presenti nel territorio del comune di Castelfranci per la costruzione di un anfiteatro. Relazione geologica-tecnica. (**in Italian, hardcopy only**)

De Vita P, Focareta M, Guadagno FM (2001) Il fenomeno franoso della località Chianiello nel Comune di Castelfranci (AV). Memorie Società Geologica Italiana 56:61–70

DM (2008) Decreto del Ministero Infrastrutture 14 gennaio 2008. Pubblicato su S.O. n. 30 alla G.U. 4 febbraio 2008, n.29. Norme tecniche per le Costruzioni. Ministero delle Infrastrutture, Ministero dell'Interno, Dipartimento della Protezione Civile. Tipografia del Genio Civile (DEI)

Dramis F, Prestininzi A, Cognini L, Genevois R, Lombardi S (1982) Surface fractures connected with the southern Italy earthquake (November 1980)—distribution and geomorphological implications. Proc 4th Int Congr of IAEG December 10–15 New Delhi India 8:55–55

EPRI (1993). Guidelines for Determining Design Ground Motions. EPRI TR-102293

Esri Italia (2010) ArcGIS for desktop (www.esritalia.it)

Fell R, Corominas J, Bonnard C, Cascini L, Leroi E, Savage WZ on behalf of the JTC-1 Joint Technical Committee on Landslides and Engineered Slopes (2008a) Guidelines for landslide susceptibility, hazard and risk zoning for land-use planning. Eng Geo 102:99–111

Fell R, Corominas J, Bonnard C, Cascini L, Leroi E, Savage WZ on behalf of the JTC-1 Joint Technical Committee on Landslides and Engineered Slopes (2008b) Guidelines for landslide susceptibility, hazard and risk zoning for land-use planning. Eng Geo 102:85–98

Franklin AG, Chang FK (1977) Earthquake resistance of earth and rock-fill dams: US. Army Corps of Engineers Waterways Experiment Station. Miscellaneous Paper S-71-17, 59 pp

GEO-SLOPE International (2004) GeoStudio suite (http://www.geo-slope.com/)

Glade T, Albini P, Frances F (eds) (2001) The Use of Historical Data in Natural Hazard Assessments. Advances in Natural and Technological Hazards Research, 17, Kluwer Academic Publishers

Goodman RE, Seed HB (1966) Earthquake-induced displacements in sand enbankments. Am Soc Civil Eng Proc J Soil Mech Found Div 92(SM2):125–146

Gringeri Pantano F, Nicoletti P, Parise M (2002) Historical and geological evidence for the seismic origin of newly recognized landslides in south-eastern Sicily, and its significance in terms of hazard. Environ Manag 29(1):116–131

Guerriero L, Revellino P, Coe JA, Focareta M, Grelle G, Albanese V, Corazza A, Guadagno FM (2013) Multi-temporal maps of the Montaguto earth flow in Southern Italy from 1954 to 2010. J Maps 9(1):135–145

Harp EL, Wilson RC (1995) Shaking intensity thresholds for rock falls and slides: evidence from the 1987 Whittier Narrows and Superstition Hills earthquake strong motion records. B Seismol Soc Am 85(6):1739–1757

Hsieh SY, Lee CT (2011) Empirical estimation of the Newmark displacement from the Arias intensity and critical acceleration. Eng Geol 122(1–2):34–42

Huang YH (1983) Stability Analysis of Earth Slopes. Van Nostrand Reinhold NY (ed)

Hutchinson JN, Prete M (1985) Landslide at calitri, southern apennines, reactivated by the earthquake of 23rd November 1980. Geologia Appl ed Idrogeol 20(1):9–28

Jibson RW (1993) Predicting earthquake-induced landslide displacements using Newmark's sliding block analysis. Transp Res Rec 1411:9–17

Jibson RW (2007) Regression models for estimating coseismic landslide displacement. Eng Geol 91:209–218

Jibson RW, Keefer DK (1993) Analysis of the seismic origin. of landslides examples from the New Madrid seismic zone. Geolo Soc Am Bull 105:521–536

Jibson RW, Harp EL, Michael JM (1998) A method for producing digital probabilistic seismic landslide hazard maps: an example from the Los Angeles, California area US Geological Survey Open-File Report 98–113, 17 p

Keefer DK (1984) Landslides caused by earthquakes. Bull Geol Soc Am 95:406–421

Keefer DK, Wilson RC (1989) Predicting earthquake- induced landslides, with emphasis on arid and semi-arid environments. In: Sadler, P.M., Morton, D.M. (Eds.), Landslides in a semi-arid environment with emphasis on the Inland Valleys of Southern California, Inland Geological Society of Southern California Publications Vol. 2, Part 1. Inland Geological Society of Southern California, Riverside CA, p 118–149

Liotti G (2010) Aggiornamento indagini geognostiche-geotecniche. Valutazioni sulle indagini effettuate e di quelle realizzate in precedenza a Castelfranci (AV). (**in italian, hardcopy only**)

Locati M, Camassi R, Stucchi M (2011) Database Macrosismico Italiano versione DBMI11

Luzi L, Pergalani F (1996) Applications of statistical and GIS techniques to slope instability zonation (1:50000 Fabriano geologic map). Soil Dyn Earthq Eng 15:83–94

Luzi L, Pergalani F (2000) A correlation between slope failures and accelerometric parameters: the 26 September 1997 earthquake (Umbria-Marche, Italy). Soil Dyn Earthq Eng 20(5–8):301–313

Menardi Noguera A, Rea G (2000) Deep structure of the Campanian-Lucanian Arc (Southern Apennine, Italy). Tectonophysics 324:239–265

Monaco L, Capobianco L (2007) Relazione Geotecnica. Lavori di messa in sicurezza del piano viabile, tratto antistante Cimitero Comunale Castelfranci (AV). (**in Italian, hardcopy only**)

Newmark NM (1965) Effects of earthquakes on dams and embankments. Geotechnique 15:139–160

Parise M (2000) Erosion rates from seismically induced landslides in Irpinia, southern Italy. In: Bromhead E, Dixon N and Ibsen ML (eds) Landslides in research, theory and practice, Proc. 8th International Symposium on Landslides, Cardiff, 3, p 1159–1164

Parise M (2001) Landslide mapping techniques and their use in the assessment of the landslide hazard. J Phys Chem of the Earth part C 26(9):697–703

Parise M, Jibson RW (2000) A seismic landslide susceptibility rating of geologic units based on analysis of characteristics of landslides triggered by the January 17, 1994, Northridge, California, earthquake. Eng Geol 58(3–4):251–270

Parise M, Wasowski J (1999) Landslide activity maps for the evaluation of landslide hazard: three case studies from Southern Italy. Nat Hazards 20(2/3):159–183

Parise M, Federico A, Palladino G (2012) Historical evolution of multi-source mudslides. In: Eberhardt E, Froese C, Turner AK, Lerouil S (eds) Landslides and Engineered Slopes. Protecting Society through Improved Understanding. Proceedings 11th Int. Symp. Landslides, Banff (Canada), 1, p 401–407

Parise M, Vennari C, Vessia G, Basso A, Tromba G (2014) Relazione finale relative alle attività dell'Istituto di Ricerca per la Protezione Idrogeologica (IRPI) per la redazione di carte tematiche di franosità del Comune di Castelfranci (AV). (in italian, hardcopy only)

Patacca E, Scandone P (2007) Geology of the Southern Apennines. Boll Soc Geol Ital Spec Issue 7:75–119

Patacca E, Sartori R, Scandone P (1990) Tyrrhenian basin and Apenninic areas: kinematic relations since Late Tortonian times. Mem Soc Geol Ital 45:425–451

Pellegrino A, Picarelli L, Urciuoli G (2003) Experiences of mudslides in Italy. In: Picarelli L (eds) Proc. Int. Workshop "Occurrence and mechanisms of flow-like landslides in natural slopes and earthfills", p 191–206

Peluso (1998) Franosità attuale ed ereditata a Castelfranci. (hardcopy only, in Italian)

Romeo R (2000) Seismically induced landslide displacements: a predictive model. Eng Geol 58:337–351

Sarma SK (1980) A simplified method for the earthquake resistant design of earth dams. Dams and Earthquakes. In: Proc. ICE Conference, London, p 155–160

Sibson R (1981) A brief description of natural neighbor interpolation. In: Barnett V (ed) Interpreting multivariate data. Wiley, Chichester, pp 21–36

Soeters R, van Westen CJ (1996) Slope instability recognition, analysis, and zonation. In: Turner AK, Schuster RL (eds) Landslides. Investigation and Mitigation. Transportation Research Board, Special Report 247, National Academy Press, Washington, p 129–177

Strenk PM, Wartman J (2011) Uncertainty in seismic slope deformation model predictions. Engr Geol 122(1–2):61–72

Tarquini S, Isola I, Favalli M, Mazzarini F, Bisson M, Pareschi MT, Boschi E (2007) TINITALY/01: a new Triangular Irregular Network of Italy. Ann Geophys-Italy 50(3):407–425

TC4-ISSMFE (1999) Manual for zonation on seismic geotechnical hazards (revised version). Published by the Japanese Geotechnical Society

Varnes DJ (1978) Slope movement types and processes. In: Schuster RL and Krizek RS (eds) Landslides-Analysis and control, chapter 2, National Academy of Sciences, Transportation Research Board Special Report 176, Whashington, p 11–33

Vessia G, Parise M, Tromba G (2013) A strategy to address the task of seismic micro-zoning in landslide-prone areas. Adv in Geosci 35:23–35

Wieczorek GF, Wison RC, Harp EL (1982) Experimental map of seismic slope stability, San Mateo County, California. US Geological Survey. Miscellaneous Investigations Series Map I-1257E, scale 1: 62500

Wieczorek GF, Wilson RC, Harp EL (1985) Map showing slope stability during earthquakes in San Mateo County, California. Miscellaneous Investigation Maps I-1257-E, USGS

Wilson RC, Keefer DK (1983) Dynamic analysis of a slope failure from the 6 August 1979 Coyote Lake, California, earthquake. B Seismol Soc Am 73(3):863–877

Yegian MK, Marciano EA, Ghahraman VG (1991) Earthquake-induced permanent deformations: probabilistic approach. J Geotech Eng-ASCE 117:35–50